NGST Phase Retrieval Camera Design and Calibration Details

Jessica A. Faust, Andrew E. Lowman, David C. Redding, Scott A. Basinger, Joseph J. Green, Catherine M. Ohara, Fang Shi
Jet Propulsion Laboratory, California Institute of Technology

ABSTRACT

Experience and infrastructure from NGST's Wavefront Control Testbed (WCT) were utilized to develop a portable wavefront sensor, the Phase Retrieval Camera (PRC). The PRC is useful for the testing of optics in high-jitter environments. The principal uses of the PRC will be testing and experimenting with NGST technology demonstration mirrors as well as exploring other issues of wavefront sensing and control not easily studied using the WCT. This presentation will detail the packaging and hardware chosen for the PRC, the PRC software, and calibration of the instrument.

Keywords: phase retrieval, NGST, wavefront control, wavefront sensing, segmented mirror

1. INTRODUCTION

The Wavefront Control Testbed (WCT) built at the Jet Propulsion Laboratory and Goddard Space Flight Center (GSFC) was designed to develop the technology and algorithms necessary to align the optics of the Next Generation Space Telescope (NGST) after its deployment. NGST technology demonstrator mirrors would benefit from testing with WCT; however, the testbed is too large and complex a system to transport to the sites where these mirrors will be tested. To solve this problem, the Phase Retrieval Camera (PRC) was constructed as a portable version of WCT (see Figure 1). This paper describes the detailed design and calibration of the PRC. A description of the wavefront sensing algorithm and experimental results can be found in reference (1).

Figure 1. Picture of the Phase Retrieval Camera on the bench

2. JITTER

2.1 Testing Environment

The NGST Mirror System Demonstrator (NMSD) and Advanced Mirror System Demonstrator (AMSD) mirrors will be tested at Marshall Space Flight Center (MSFC) in the X-Ray Calibration Facility (XRCF). The facility lacks the vibration isolation that is typical of optical test facilities. When the PRC development began, the Wavefront Sensing and Control (WFS&C) working group at GSFC developed an experiment to determine the extent of the jitter at the MSFC facility[2]. Image jitter was measured at the center of curvature of a 19m mirror. The results of this test showed that jitter was on the order of 10-12 microns rms (horizontal) and 4-5 microns rms (vertical). The jitter rate was less than 5 microns/ms 90% of the time. Conventional interferometers fail in this sort of high jitter environment and specialized interferometers are needed for the optical testing.

2.2 Solutions to Jitter Problem

Because of the jitter, a fast steering mirror (FSM) was considered for the PRC but it was concluded that it would be too complicated and costly. An FSM would also have had an impact on the packaging, possibly limiting the portability of the instrument. The alternative that was chosen was to use a high speed shutter and a laser diode source. The high speed shutter is capable of a minimum exposure time of 0.3 ms and does reduce the jitter that would be seen in the XRCF to an acceptable level most of the time. The laser diode provides a high signal-to-noise (SNR) source for the very short exposures that the high speed shutter takes.

To further reduce the jitter's impact on the measurements, dual cameras were used in the design (see Figure 2). The first camera is for wavefront sensing (WFS) and the second is a reference for calculating the centroid of the image, giving us a measurement of the jitter so that it can be compensated for during the data analysis. The reference camera provides an in-focus image, the displacement of which is magnified by a factor of 4 relative to the WFS camera. This allows for boresighting of the WFS camera images to a high degree of accuracy. Typically, several data frames are averaged for each defocus position during a measurement. By monitoring the size of the in-focus reference images, frame selection can be employed to remove images for which the shutter speed was inadequate.

As higher levels of WFS accuracy are required, the reference camera may not offer sufficiently accurate signals for co-registering an ensemble of defocused point spread function (PSF) measurements. Residual mismatches in the true center of the defocused PSF measurements as compared to the presumed optical axis induce error in to our WFS. As it has recently been shown, this error can exceed $\lambda/100$ rms for centering errors of a half of a Nyquist pixel[3].

To overcome this limitation, a novel image based approach for centering defocused PSF images was developed. In this approach, Fourier methods are used for shifting the PSF with sub-pixel accuracy. For each level of defocus, the optical transfer function (OTF) is computed by taking the Fourier transform of the measured PSF. The tilt in the phase of the OTF is then estimated. This tilt is directly related to the PSF center offset[4]. The conjugate of this phase term is computed and applied back to the OTF to correct the center offset. Finally, taking the inverse Fourier transform of the OTF produces a more centered PSF. By iterating this process, an ensemble of defocused PSF can be brought into alignment with the presumed optical axis.

This centering method was applied in study validating the PRC WFS accuracy to very high level[5]. In this study, PRC optical path difference (OPD) estimates were directly compared to Zygo interferometer measurements and were found to agree to the level of 4nm rms at 675nm, which was on the level of uncertainty in this experiment. Part of this success is attributable to the accurate PSF centering performance of the OTF based approach.

3. SENSOR MODULE

The PRC sits on an 18 inch by 24 inch breadboard. The package was designed to be approximately the same size as a Zygo interferometer. The breadboard is 0.5 inch thick. Because of the weight of the component parts that are on the breadboard, a stiffener plate was added to the bottom. The stiffener is also a 18 inch by 24 inch by 0.5 inch breadboard. Figure 2 is the mechanical layout of the PRC and Figure 3 is a simple diagram of the light path of the PRC. The incoming light source is provided by a single mode fiber with an angle polish. This reflects the returning beam and

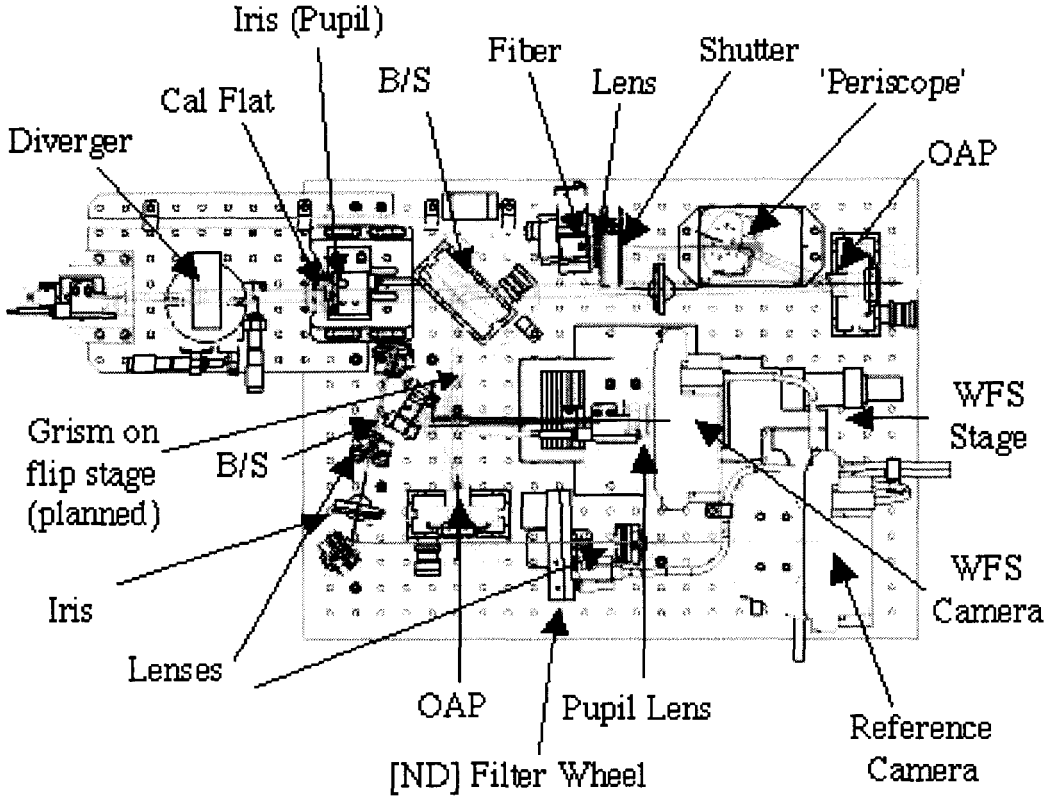

Figure 2. Mechanical Layout of the PRC Sensor Module.

prevents it from reaching the cameras as a ghost image. The fiber is followed by a high-speed Uniblitz® shutter which provides exposure times as fast as 1 msec in regular operation mode and 0.3 msec in high-speed mode. The diameter of shutter is 1 mm. The light leaving the fiber is imaged on the shutter using a lens, thus preventing clipping of the beam that would lead to diffraction artifacts. Some concerns about the shutter potentially causing jitter on the sensor module have lead to the decision to move the source module to the entrance of the fiber instead of the exit. This will occur when a new source module is constructed.

The shutter is then followed by an off-axis parabolic (OAP) mirror to collimate the diverging beam. The collimated beam then passes through a beamsplitter (B/S) designed to cover the laser diode wavelengths that have been chosen for the source module. The beamsplitter is anit-reflection (AR) coated and wedged approximately 1 degree so that a dual reflection ghost beam will fall off of the CCD camera. The beam reflected off of the beamsplitter is sent to a beam dump and the transmitted beam continues on through the system.

The transmitted beam passes through an iris positioned at the pupil plane. To simplify the phase retrieval process, it is important that the system be telecentric in image space. Thus the diverger lens that is chosen to match the collimated beam to the test optic must also image the test optic (considered the stop) onto this aperture, and the iris is located at the front focal point of the focusing OAP. Immediately following the iris is a calibration flat mounted on a New Focus® flipper mechanism. This enables the measurement of the internal aberrations of the PRC for calibration purposes. The diverger sits on a removeable plate. This design feature was added to keep the packaging of the sensor module to the footprint of the breadboard.

The beam returning from the test optic passes through the diverger lens again and strikes the beamsplitter where the transmitted beam returns along the path to the fiber and is reflected off of the angle-polished tip. The reflected beam continues on through the sensor module. The dispersed fringe sensor (DFS) mechanism, comprised of a grating prism (grism) in another New Focus® flipper, is situated in the collimated beam after the beamsplitter and before the focusing OAP. The grism has not yet been added to the system. The OAP focal length together with the aperture diameter ensures Nyquist sampled images on the WFS camera.

The converging beam then strikes a small beamsplitter that separates the beam into the WFS and reference arms of the system. This beamsplitter is wedged to minimize the astigmatism in the beam transmitted into the reference arm. The reflected beam continues onto the WFS camera. A Photometrics SenSys® science grade CCD camera is used. The camera is mounted on a Newport motorized translation stage which is capable of 100 mm of motion, thus providing ±50 mm of defocus. A New Focus® flipper is mounted in front of the camera (on the stage) and contains a small imaging lens to provide a pupil image at the WFS camera. A stock doublet was chosen for the imaging lens to minimize pupil distortion.

The transmitted beam is then folded and hits a collimating lens (a singlet). Next the beam passes through an iris and strikes another fold mirror. The next element in the path is the filter wheel. Low wedge neutral density filters are used to attenuate the beam without shifting the spot. The source must be made brighter when the WFS stage is used to defocus the image. When this occurs, the unattenuated reference beam would saturate the reference CCD. The filter wheel is slightly tilted so that the reflected beam is blocked by the iris previously mentioned; this prevents the ghost image from propogating backward through the entire system. The beam is then re-focused by another lens which provides a magnification of 4 for the reference camera. The reference camera is identical to the WFS camera and sits on a manual translation stage. The diffraction limited depth of focus is ±12.5 mm. The focus position of the camera must be much more accurate than that to minimize the spot shift as the filters are inserted, so a large glass block is tilted in the collimated beam during alignment as an aid in finding the best focus.

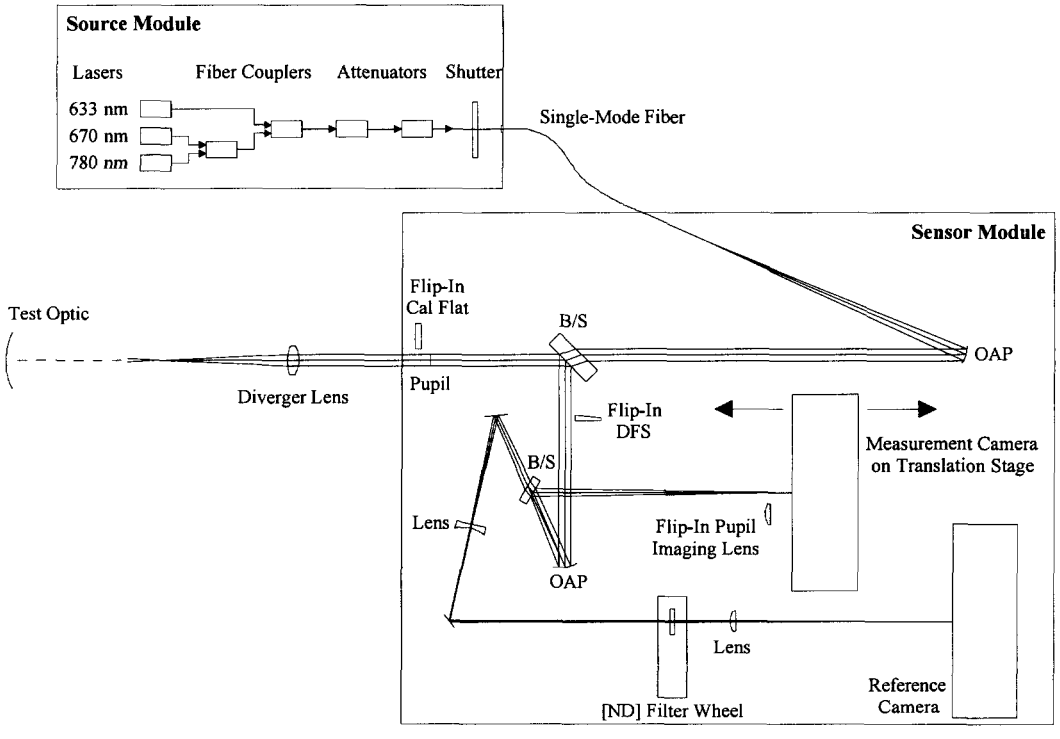

Figure 3. Simplified diagram of the sensor and source modules of the PRC and the light path.

4. SOURCE MODULES

There are two source modules for the PRC: a laser source module and a white light source (WLS) module. See Figure 3 for a layout of the laser source module. A single mode fiber is coupled to the proper source module for the mode of operation to be used. The fiber transmits the light to the sensor module. The WLS will be discussed in the next section on the DFS.

The laser source module contains one 670 nm laser diode at present. It will soon be expanded to include another laser diode with a wavelength of 780 nm and an externally coupled Helium-Neon laser source. The He-Ne source is being added to match the design wavelength of the computer generated hologram (CGH) that will be used to null test AMSD mirrors. While one laser diode is sufficient for phase retrieval, two laser diodes were chosen such that their wavelength separation was large enough to resolve a step (i.e. a piston measurement) for a segmented mirror system.

The laser sources are coupled to fiber attenuators which are tuned for their wavelength range. There are two attentuators for each laser. The He-Ne laser and the 670 nm diode will share an attenuator set; their wavelengths are close enough to make it unnecessary to have a third set of attentuators. The attenuators are used to control the source flux and work by blocking the beam as it passes through. When the WFS camera is in focus, the ability to reduce the flux is essential or else saturation of the camera is inevitable. However, as the camera is defocused and light is spread out over more of the CCD, the source attentuation must be decreased to maintain the same SNR level.

At this point, in the current source module, the output of the attenuators is coupled directly to the output fiber. In the new source module, the output from each attenuator set will be directed into a beam combiner. The high-speed shutter that is currently part of the measurement module will be inserted after the beam combiner. The output will then be coupled to the single mode fiber that propogates the beam to the measurement module.

5. DISPERSED FRINGE SENSOR

Dispersed fringe sensing is a technique for detecting large piston errors in segmented mirror optics. As part of the NGST baseline wavefront sensing and control methodology, it has demonstrated excellent performance in phasing the segmented aperture system on the WCT, successfully correcting initial piston aberrations (sometimes as large as 1 depth-of-focus) to better than 200 nm[6]. The DFS will be used during a phasing experiment involving an AMSD mirror segment and a fixed reference segment at the MSFC XRCF facility. The DFS method requires a broadband light source that will be provided by the PRC WLS module.

The WLS uses a Xenon lamp and optics to image the beam into the single mode fiber. A motorized filter contains narrowband filters for calibration of the DFS and another high-speed shutter is used in the path to control exposure times and jitter.

When the DFS method is being used the grism is flipped into the optical path. Two transmissive grisms were procured to be used as the dispersing element, one with 35 lines/mm and the other with 75 lines/mm. The choice of line densities is determined by the dynamic range of the piston. The grism disperses the light from the WLS by wavelength thus forming a spectrum on the CCD. The grism can be manually rotated in its mount to change the contrast (or visiblity) of the fringes.

6. COMPUTERS AND ELECTRONICS

The hardware is controlled by a personal computer (PC) called the Optics Control Computer (OCC). The OCC runs Windows NT and has dual-processors. It contains two Photometrics framegrabber cards (one for each camera), a National Instruments Data Acquisition (DAQ) board, and an 8-port multiple serial port board. The serial ports are used to drive the two attenuators, the Newport motion controller (for the motorized stage), the motorized filter wheels, and an uninterruptable power suppy (UPS). The DAQ board includes analog output lines that control the power level of the lasers, a timer signal to drive the shutter, and digital input/output (I/O) lines to drive the flippers. The PRC computer and electronics are rack-mounted for portability, as shown in Figure 4.

A Beowulf system consisting of two dual-processor rack-mounted PCs running Linux and distributed processing software are used for running experiments and numerical computations. For the most part, experiments are run remotely over the internet. However, the Beowulf provides a standalone capability for testing and processing when no network access is available.

7. SOFTWARE

The PRC OCC software was written using National Instruments Labwindows/CVI® and is based on the OCC software written for the larger WCT. The graphical user interface (GUI) allows the user to control all functions of the hardware components (see Figure 5). The OCC program utilizes a network interface using Tranmission Control Protocol (TCP) sockets. This interface allows for remote control via the internet. The PRC OCC software consists of a server and a client. The server must be running to allow for remote or local control of the PRC. The OCC GUI allows the user to access all functions of the PRC and is used in the alignment process. For example, during alignment of the system, it is useful to open the shutter to allow the source beam to be visible on the test optic. The video mode is useful during alignment of the sensor module internally and alignment of the diverger and test optic.

The PRC Segmented Telescope Control Software (STCS) is a software package derived from the STCS[7] [7]used on the WCT (see Figure 6). It is used for the actual measurement and experimental work to acquire phase retrieval data and determine the wavefront errors on the test optic being measured. The STCS is written in the Math Works Matlab® and runs on a remote system from the PRC electronics rack. The experimenter runs the GUI and uses it to set up the controls for a measurement. For a typical experiment, several out-of-focus images and a pupil image are required to run the phase retrieval algorithm[8]. Each image has several unique settings for filter wheels and

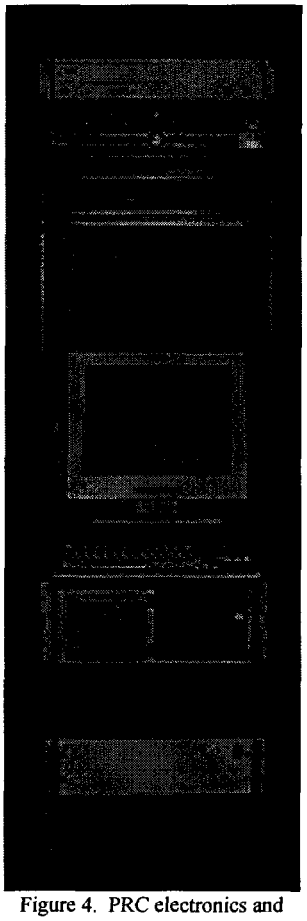

Figure 4. PRC electronics and computer

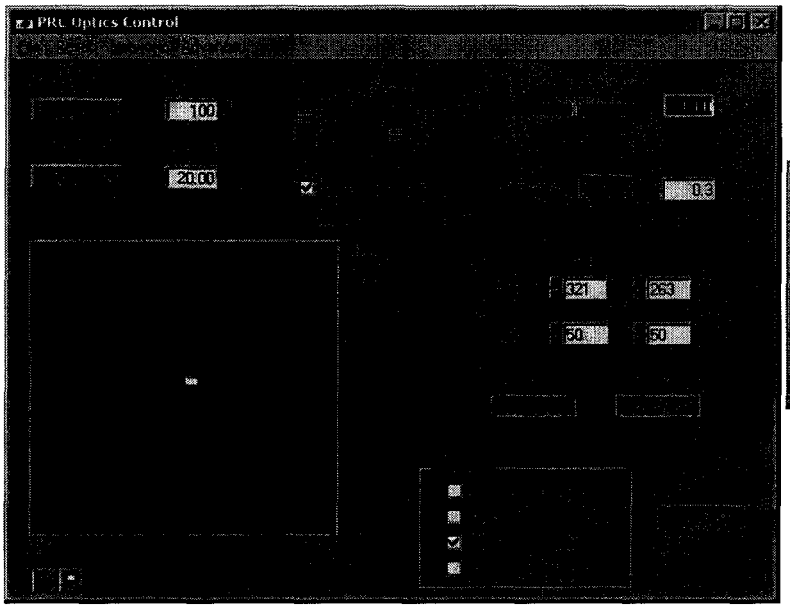

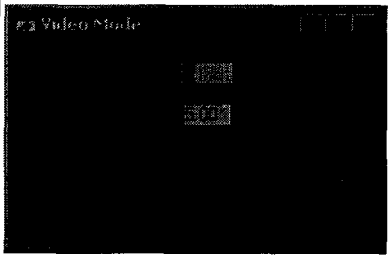

Figure 5. PRC OCC Client used for local control on the PRC (left) and Video Mode controls (right)

various other moving parts on the testbed. The STCS sends commands to the PRC OCC over the network to change the hardware configurations and displays the images when they are returned.

8. CALIBRATION

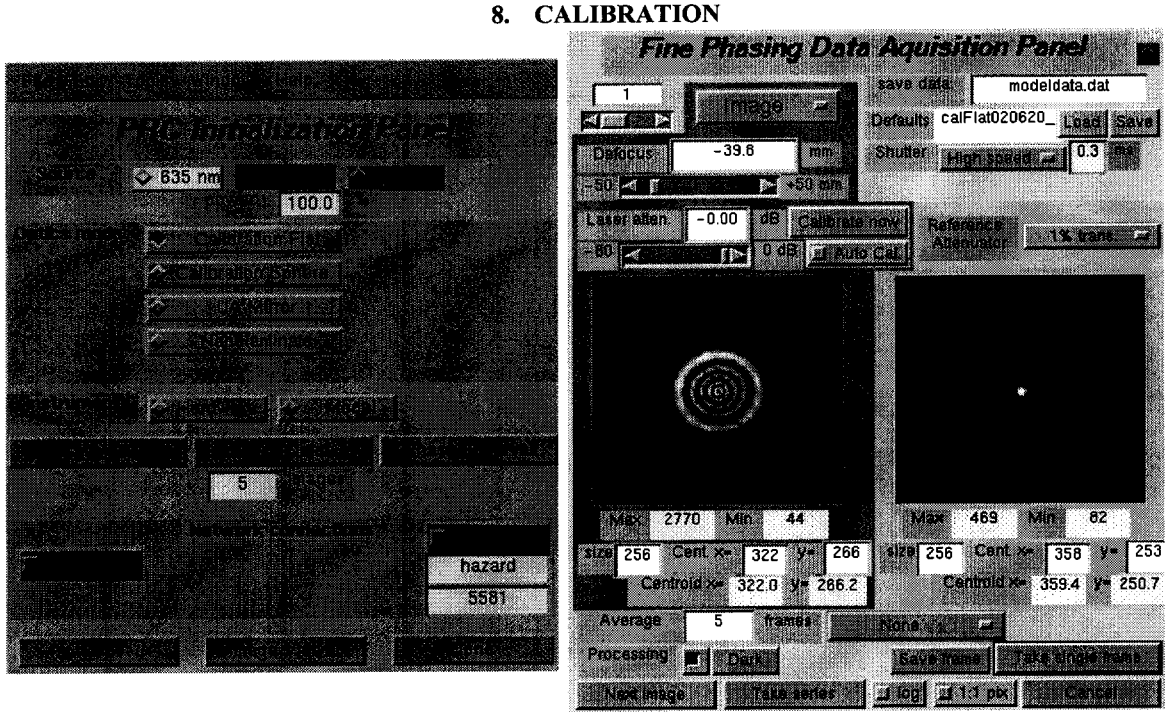

Figure 6 PRC STCS Configuration Panel (left) and Data Acquisition Panel (right)

8.1 Reference Camera Magnification and Alignment to the WFS Camera

The image of the PSF in the reference camera is nominally magnified by a factor of four. In order to determine the value of this magnification an experiment was performed comparing the centroid positions in both cameras using the calibration flat and an external flat mirror. In Figure 7, 250 measurements were taken with the calibration flat in the

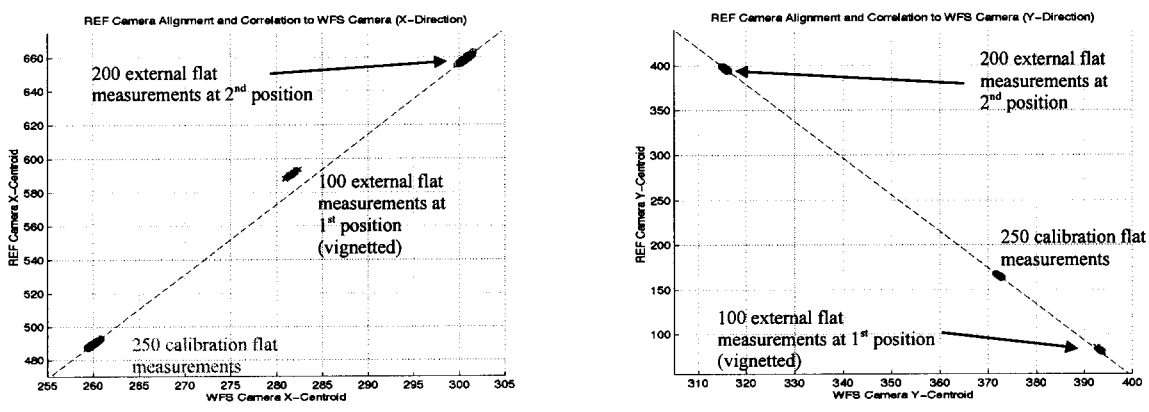

Figure 7. Reference camera magnification calibration plots: X-centroids (right) and Y-centroids (left)

beam path and 100 measurements were taken with a tilted external calibration flat. Then it was determined that the external flat was vignetted and 200 more measurements were taken with the external flat aligned at another position. In Figure 7, the two plots show the three sets of measurements with the WFS x-centroid compared to the reference x-centroid and a similar plot for the y-centroids. The centroid pairs correlated to better than 99% over the combined calibration flat and external flat measurement ensemble. By comparing the centroid values of the WFS and reference cameras, it can be seen that the magnification is approximately 4.

8.2 System F/#

To calibrate the f/# of the optical system, measurements are taken to directly observe the optical cutoff frequency. In Figure 8, a defocused PSF image taken with the stage set at +7.5 mm is shown along with its Fourier transform. The location of the optical cutoff frequency indicates that the system is about 4% undersampled with the fixed aperture. Knowing the imaging wavelength (λ = 675.5 nm) and the camera pixel size (9 microns) allows computation of the f/#. The f/# calculates to be approximately 25.5.

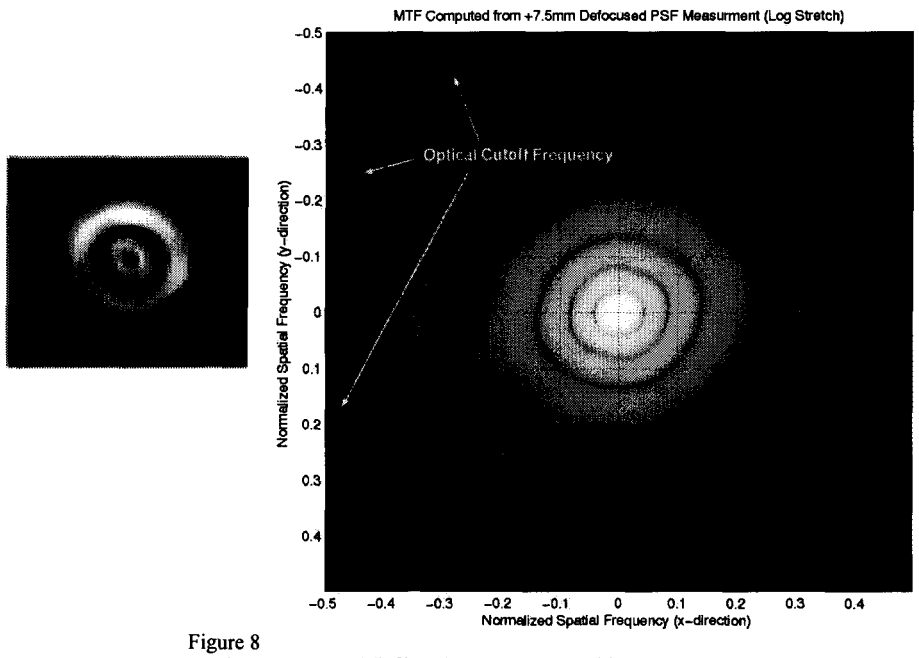

Figure 8
frames co-added (left) and computed MTF (right)

8.3 Best Focus Position for the WFS Camera

Best focus refers to the WFS camera stage position that minimizes the defocus aberration in the apparent system pupil. A sequence of defocused PSF measurements is taken about the approximate best focus with the calibration flat in place to calibrate the absolute focus position. The measurement sequence is then given to Modified Gerchberg-Saxton (MGS) algorithm[8] to estimate the system OPD. Any residual defocus aberration is an indication in the offset of absolute focus and the approximated best focus. With the calibration of the system F/#, the stage position that is at the absolute best focus of the system can easily be computed.

Table 1 contains the calibration values of various system parameters, including those mentioned above.

System Parameter	Calibrated Value
Exit Pupil Location	Infinity (Telecentric)
F/#	25.5 (with fixed stop)
Sampling at λ=675.5nm	4.3% undersampled (λ=675.5nm, 9μm pixels)
Best Focus Position	+0.10 mm
Induced defocus aberration by translation	-0.285 waves/mm
Internal optical aberrations	5.8 nm rms wavefront 70.0 nm p-v wavefront
Reference Camera Magnification (due to PSF magnifier)	$m_x = +4.155$ $m_y = -4.086$
Reference Camera LOS Jitter (low-frequency)	0.82 pixels (1-σ, Gaussian model)
WFS Camera Alignment Offset (due to translation)	$t_x = 0.053$ pixels/mm $t_y = 0.026$ pixels/mm
WFS Camera LOS Jitter (low-frequency)	0.20 pixels (1-σ, Gaussian model)
WFS Camera LOS Jitter (high-frequency, blur)	$\sigma_x = 0.55$ pixels $\sigma_y = 0.62$ pixels

Table 1. Calibrated System Parameters

9. ONGOING WORK

The WLS is currently being assembled and aligned. In addition, the new laser source module is in the final stages of design and fabrication. The PRC will be used to test the NMSD mirror at the University of Arizona and at MSFC in the XRCF facility. AMSD mirrors will also be tested with the PRC at MSFC during both the individual mirror tests and a two mirror phasing test. In the future, it will be used for testing other NGST optics as well as other projects as needed.

ACKNOWLEDGEMENTS

This research was carried out at the Jet Propulsion Laboratory, California Institute of Technology, under a contract with the National Aeronautics and Space Administration.

REFERENCES

1. A. E. Lowman, D. C. Redding, S. A. Basinger, D. Cohen, J. A. Faust, J. J. Green, C. M. Ohara, and F. Shi, "Phase Retrieval Camera for Testing NGST Optics", SPIE vol. 4850 (Waikoloa, 2002).
2. M. Fitzmaurice, T. Norton, P. Petrone III, J. Schott, "Results of optical jitter tests at the MSFC X-Ray Calibration Facility," internal Goddard Space Flight Center report (25 Oct 2000).
3. J. J. Green, D. C. Redding, S. Shaklan and S. A. Basinger,"Extreme Wave Front Sensing Accuracy for the Eclipse Coronagraphic Space Telescope," Proc. SPIE vol. 4860 (Waikoloa 2002).
4. J. D. Gaskill, Linear Systems, *Fourier Transforms, and Optics*, John Wiley & Sons, New York, 1978.
5. J. J. Green, D. C. Redding, Y. Beregovski, A.E. Lowman, and C.M. Ohara, "Interferometric validation of image based wavefront sensing for NGST," Proc. SPIE vol. 4854 (Waikoloa 2002).
6. F. Shi, D. C. Redding, A. E. Lowman, C. W. Bowers, L. A. Burns, P. Petrone III, C. M. Ohara, and S. A. Basinger, "Segmented Mirror Coarse Phasing with a Dispersed Fringe Sensor: Experiment on NGST's Wavefront Control Testbed", SPIE vol. 4850 (Waikoloa, 2002).
7. S. A. Basinger, D. C. Redding, F. Shi, D. Cohen, J. J. Green, C. M. Ohara, A. E. Lowman, and L. A. Burns, "Wavefront sensing and control software for a segmented space telescope," SPIE vol. 4850 (Waikoloa, 2002).
8. S. A. Basinger, D. C. Redding, A. E. Lowman, L. A. Burns, K. Liu and D. Cohen, "Performance of wavefront sensing and control algorithms on a segmented telescope testbed," Proc. SPIE, *UV, Optical and IR Space Telescopes and Instruments*, V 4013, pp. 749-756 (2000).